J Nanostruct 15(3): 1009-1024, Summer 2025

RESEARCH PAPER

Study of Thermal Conductivity Coefficient, Mechanical, True Density, Apparent Porosity, and Water Absorbance Properties of [PVA:PEO-$CuCl_2.2H_2O$] Composite

Zena Jabber Salih *, Sabah Anwer Salman

Department of Physics, College of Science, University of Diyala, Iraq

ARTICLE INFO

Article History:
Received 24 March 2025
Accepted 19 June 2025
Published 01 July 2025

Keywords:
[PVA:PEO] blend
Composite films
$CuCl_2.2H_2O$ salt

ABSTRACT

Blended films of polyvinyl alcohol and polyethylene oxide reinforced with $CuCl_2.2H_2O$ (10–50 wt%) were prepared using the solution casting technique to investigate the impact of salt concentration on structural, thermal, mechanical, and physical properties. Experimental results revealed that the thermal conductivity coefficient initially increased with rising salt content, then decreased at intermediate concentrations, and subsequently increased again at higher salt ratios. This non-linear trend suggests structural modifications due to interactions between PVA, PEO, and $CuCl_2.2H_2O$, which altered the films' internal morphology. For mechanical properties, irregular behavior was observed in hardness, impact resistance, and tensile strength as the salt ratio increased. Fracture energy and impact toughness exhibited inconsistent trends, while elongation at break fluctuated unpredictably, reflecting changes in the films' flexibility and structural cohesion. Physically, the true density of the films initially decreased and then increased with higher salt content. Apparent porosity first declined but later rose irregularly, whereas water absorption decreased initially before increasing steadily with salt addition. These trends indicate that $CuCl_2.2H_2O$ influences polymer network formation, potentially enhancing or disrupting intermolecular bonds depending on its concentration. The study confirmed chemical interactions between PVA, PEO, and $CuCl_2.2H_2O$, which directly affected the films' properties. The non-linear relationship between property and salt concentration highlights the need for further optimization studies to determine ideal ratios for specific practical applications.

How to cite this article
Salih Z., Salman S. Study of Thermal Conductivity Coefficient, Mechanical, True Density, Apparent Porosity, and Water Absorbance Properties of [PVA:PEO-$CuCl_2.2H_2O$] Composite. J Nanostruct, 2025; 15(3):1009-1024. DOI: 10.22052/JNS.2025.03.018

INTRODUCTION

Polymers are vital materials in contemporary industries due to their advantageous that surpass those of traditional materials, along with the economical production of various variants, as they are resistant to rust and corrosion, lightweight, and possess commendable mechanical properties [1]. Polymers have infiltrated the production of various industrial materials, including children's toys, automotive bodies, and aircraft. Their applications have also expanded for the fabrication of solar cells and chemical cells. Insulators, like polymers, are used to make electronic circuit boards,

* *Corresponding Author Email: zenajsalih@gmail.com*

electrical insulation, and wire and connector coatings. Insulating qualities of most polymers make them suitable for various applications due to high-temperature and stress resistance. Polymers are organic compounds composed of elongated molecules formed by the repetition of one or more types of tiny units known as monomers, which serve as the fundamental building blocks of the polymer. Polymers exhibit several characteristics [2, 3], including (i) easy molding, i.e. it does not require post-processing, (ii) Low density, high specific resistance, and significant corrosion resistance render them crucial for applications without high mechanical strength, (iii) Low thermal conductivity and low thermal expansion coefficient as compared to metals, (iv) Low moisture absorption and good electrical properties, (v) They are colorfast and transparent, so they are used as an alternative to glass in some applications. But with all these advantages, they have some disadvantages, namely, low elasticity modulus and low durability at low temperatures. The connection bonds in polymer molecules are categorized in covalent bonds (Covalent Bonds) and internal partial forces called Vander Waals forces. So polymer structures depend on the shape of the chains [3, 4], as described below:

1. Linear polymers:

The structural units in these polymers are connected to each other in a continuous linear manner, and the bonding forces between the bonds are Van der Waals bonding forces, and these polymers are more crystallizable than other polymer types and have desirable mechanical properties.

2. Cross-linked polymers:

The binding forces that connect the chains in these polymers are covalent bonding forces, and are sometimes achieved by adding atoms or molecules that in turn form a covalent bond between the chains. Degree of entanglement has great impact on the mechanical and physical properties. For example; as a degree of entanglement increases and rubbery qualities decrease.

3. Branched polymers:

Branched polymers such as polystyrene and polypropylene consist of side branches and are related to the main chain. These branches can occur in linear polymers or any other type of polymers.

4. Ladder polymers:

These polymers consist of two chains of linear polymers linked in a regular manner and have less stiff than their linear counterparts.

5. Network polymers:

These are three-dimensional networks such

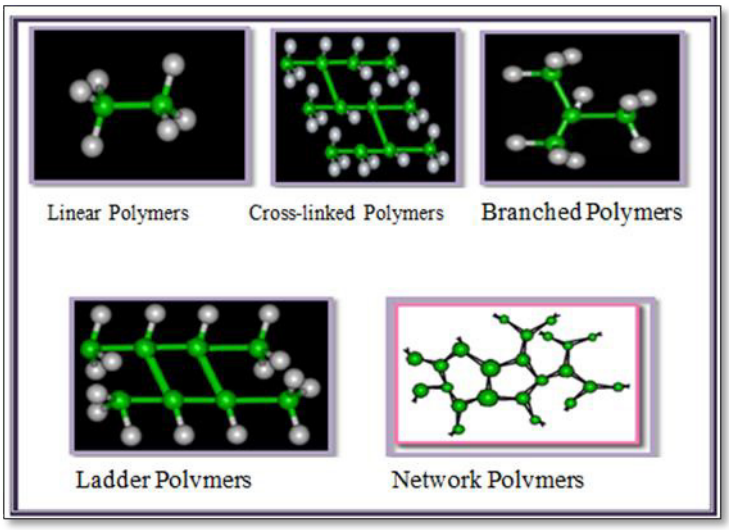

Fig. 1. Various types of chain architectures for polymers [2].

as epoxy and phenol-formaldehyde that contain a high degree of crosslinking to provide hardness and strength [2, 3]. Fig. 1 shows the types of polymer structures [2].

MATERIALS AND METHODS

Polyvinyl alcohol (PVA)

It is non-toxic white powder that dissolves rapidly in distilled water. It is a product with an average molecular weight between 13000 and 23000 g/mol that is soluble in water after extension. PVA has a viscosity of 4% in water, its loss after drying is 5%, and the residue after ignition is 0.9% and its pH ranges from 4.5 to 6.5. It has a glass transition (T_g) at 85℃ and dissolves in hot distilled water when heated at a temperature

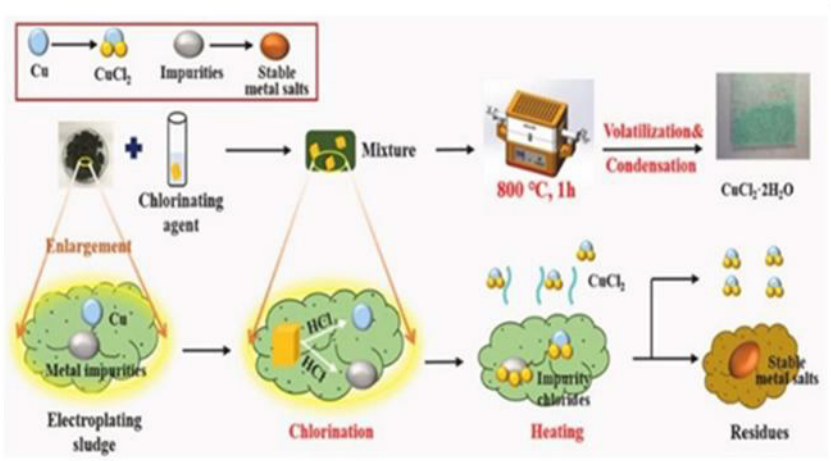

Fig. 2. A schematic representation of the procedure for obtaining $CuCl_2.2H_2O$ [6].

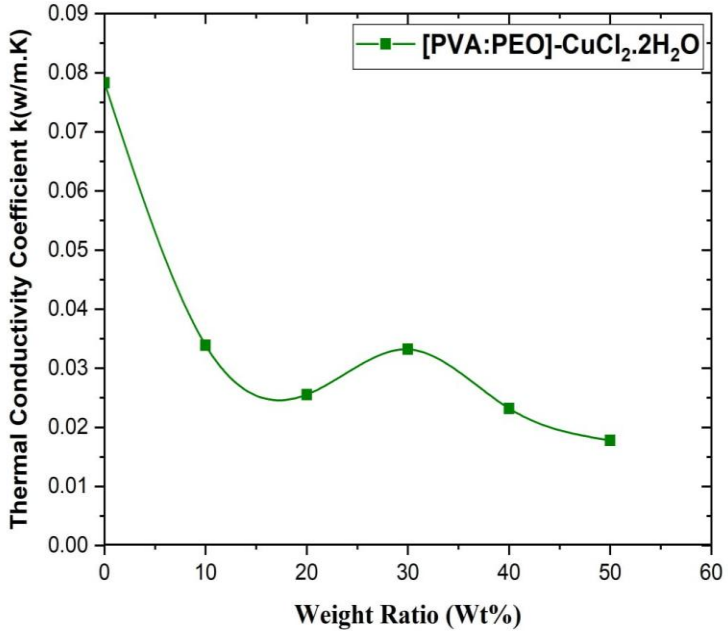

Fig. 3. Thermal conductivity coefficient of pure [PVA:PEO] blend film and the films reinforced with $CuCl_2.2H_2O$ at different weight ratios.

of 80°C and low solubility in ethanol, and has a high melting point of 2300°C.

Polyethylene oxide (PEO)

Developed by Cheng Du Micxy Chemical Co Ltd, the polymer known as polyethylene oxide is made through the polymerization of ethylene oxide, resulting in a diverse molecular weight range from 150,000 to 10 million. With versatile nature, it has a softening point ranging from 65 to 67 °C, its apparent density is 0.2~0.3 kg/L and its true density is 1.15~1.22 kg/L. It is considered in the field of polymer chemistry, characterized by a molecular mass greater than 20,000 g/mol and is either in liquid or solid form with a low melting point depending on its molecular weight. It is also used in many industrial applications [5].

Reinforcement material

Copper chloride ($CuCl_2.2H_2O$)

It is a chemical compound with the molecular formula of $CuCl_2.2H_2O$ additive. It is found naturally in minerals and its molecular weight is 170.48 g/mol. It is in the form of green crystals called dihydrate that dissolves in water and its solubility is 75.7 g per 100 mL of water. $CuCl_2.2H_2O$ is weakly soluble in acetone and diethyl ether, its molar mass is 134.45 g/mol when free of water. It has a high polarization property and contains maximum impurities of sulfur compounds (SO_4) of 0.1% and hydrogen sulfide (1%). Fig. 2 records a schematic representation for preparation of $CuCl_2.2H_2O$ [6].

Preparation of composites

A homogeneous mixture was created by combining the specified weight ratio of PVA and PEO in 30 mL of distilled water, followed by magnetically stirring for 3 h at a temperature range of 60–70 °C. The objective was to produce pure [PVA:PEO] blend films based on $CuCl_2.2H_2O$ (10- 50 wt%). After that, the mixture was carefully transferred into specialized glass moulds that were placed on a level surface. The moulds were then placed in a dark to dry.

RESULTS AND DISCUSSION

Thermal conductivity

The thermal conductivity coefficient (k) was calculated using Lees Dissc method based on Eqs .1 and 2, respectively [7].

where, e represents the amount of thermal energy passing through a unit area of the disc material per second (W/m². K).

where, T_A, T_B, and T_C (°C)shows temperatures of discs (A, B, C), respectively. d (m) is thickness of the disc. r (m) is radius of the disc. I (A) shows current passing through the heater coil in amperes. V (V) is voltage across the heater coil in volts.

Fig. 3 shows a thermal conductivity coefficient of the pure [PVA:PEO] blend film and the polymeric blend film reinforced with $CuCl_2.2H_2O$ salt in different weight ratios. It is observed that the thermal conductivity coefficient value of the pure blend film [PVA:PEO] is 0.0783W/m.K. When reinforcement with $CuCl_2.2H_2O$ at different weight ratios, the thermal conductivity coefficient value decreases irregularly with an increase in the weight ratio of added $CuCl_2.2H_2O$. The irregularity in this value is attributed to the independent behavior of thermal conductivity coefficient

$$k\left((T_B-T_A)/ds\right) = e\left[T_{A+}2/r\left(d_{A+}1/4\,ds\right)T_{A+}1/2r\,ds\,T_B\right] \quad (1)$$

$$IV = \pi r^2 e\left(T_{A+}T_B\right) + 2\pi r e\left[d_A T_{A+} ds/2\left(T_{A+}T_B\right) + d_B T_B + d_C T_C\right] \quad (2)$$

Table 1. The values of the thermal conductivity of pure [PVA:PEO] blend film and the films reinforced with $CuCl_2.2H_2O$ at different weight ratios.

Weight ratio of additive salt $CuCl_2.2H_2O$ (wt%)	[PVA:PEO]-$CuCl_2.2H_2O$ k (W/m.K)
Pure [PVA:PEO]	0.0783
10	0.0338
20	0.0255
30	0.0332
40	0.0232
50	0.0177

against the heat capacity [7-9]. The decrease in the thermal conductivity of the reinforced films as compared to the pure [PVA:PEO] blend film is attributed to the lack of homogeneity between the [PVA:PEO] matrix material and the reinforced $CuCl_2.2H_2O$. Additionally, the thermal conductivity

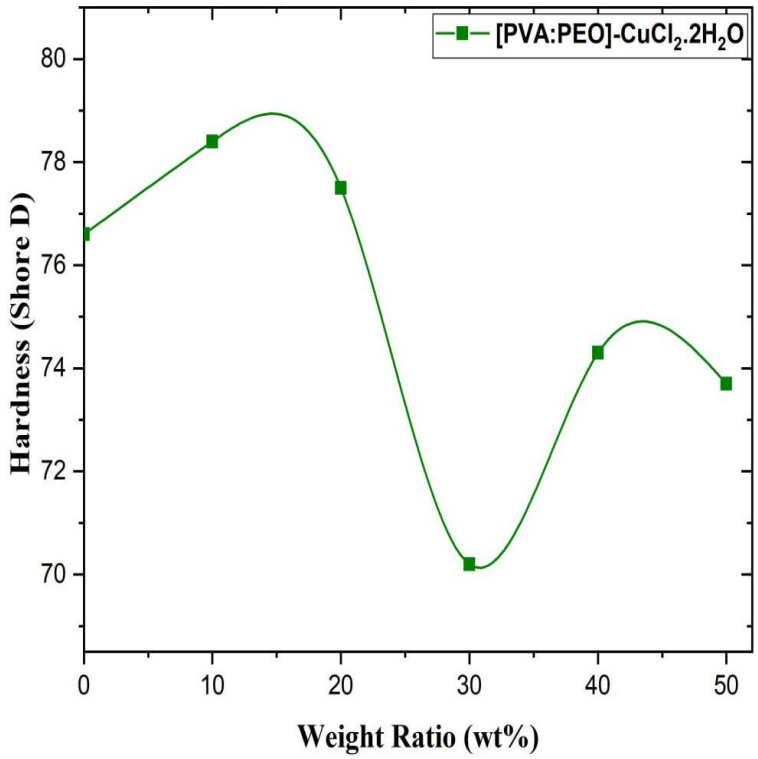

Fig. 4. Hardness of pure [PVA:PEO] blend film and the films reinforced with $CuCl_2.2H_2O$ at different weight ratios.

Table 2. The value of the hardness of pure [PVA:PEO] blend film and the films reinforced with $CuCl_2.2H_2O$ at different weight ratios.

Weight ratio of additive salt $CuCl_2.2H_2O$ (wt%)	[PVA:PEO]-$CuCl_2.2H_2O$ Hardness
pure [PVA:PEO]	76.6
10	78.4
20	77.5
30	70.2
40	74.3
50	73.7

becomes unstable due to the surface area of the salt [10-12], according to the research [13]. This phenomenon can be due to the deviation from the crystalline ratio in pure polymers of PVA and PEO [14, 15]. Photons that pass rapidly and in sufficient numbers through a crystalline structure will expand the crystalline lattice into an amorphous structure, causing the photons to scatter into irregular paths in different directions, which leads to an overall decrease in thermal conductivity on the surface, specifically in the semi-crystalline part [13, 16, 17]. Table 1 shows the thermal conductivity coefficient values for all the polymeric blend films.

Mechanical properties

The hardness (Shore D) was measured for the pure [PVA:PEO] blend film and blend films reinforced with different weight ratios of the $CuCl_2.2H_2O$, as shown in Fig. 4 and Table 2. It is observed that the hardness of the pure [PVA:PEO] is 76.6. After reinforcement with $CuCl_2.2H_2O$ at different weight ratios, the hardness increased, reaching its maximum value of 78.4 at 10 wt% of $CuCl_2.2H_2O$. Subsequently, the hardness decreased irregularly with increasing the weight ratio of the added $CuCl_2.2H_2O$. Hardness is the plastic deformation of material under external stress. When polymers are blended, the hardness of the material increases. This is attributed to the increased cross-linking and packing, which reduces the movement of polymer molecules, thereby enhancing the material's resistance to scratching or cutting and increasing its resistance to plastic deformation [18, 19]. Additionally, the reinforcement material penetrates into matrix material and the interstitial spaces and voids, increasing the contact area and forming a stronger bond between the matrix material and the reinforcement. This enhances the composite's hardness [20]. Hardness depends on the type of forces that bind the molecules or atoms within the material; stronger binding forces result in increased hardness. Therefore, strong bonding at the interfaces of the polymers and increased cross-linking in polymer blend creates a closed space that enhances hardness. This is evident at the 10 wt% of salt. Conversely, the irregular decrease in hardness is attributed to the increased viscosity acquired by the composite material from the polymeric blend with different weight ratios of $CuCl_2.2H_2O$ added to the [PVA:PEO] matrix material in its liquid state. The difficulty for $CuCl_2.2H_2O$ for diffusion into interstitial spaces of the polymer leads to the formation of numerous voids within the prepared composite material upon solidification, which in turn reduces the hardness.

The fracture energy and impact strength were measured using the free-falling body method, as below [21]:

$$I.S = E/A \quad (3)$$

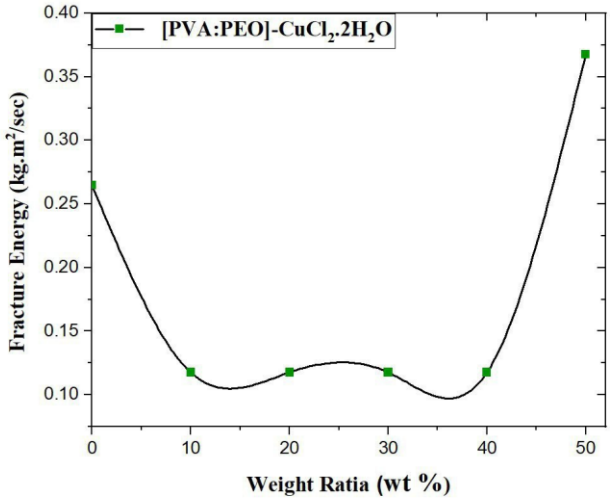

Fig. 5. Fracture energy of pure [PVA:PEO] blend film and the films reinforced with $CuCl_2.2H_2O$ salt at different weight ratios.

where, I.S is impact strength (KJ/m²). E shows fracture energy (KJ). A is cross-sectional area (m²).

The falling weight impact test is performed by freely dropping an impactor from a known height [22, 23]. The fracture energy (E) in this case can be calculated from the following relationship [22]:

$$E = mg\,h \quad (4)$$

where, m is mass of the weight (kg). g shows gravitational acceleration (9.806 m/sec²). h represents falling distance (m).

As illustrated in Figs. 5 and 6, it was observed that the fracture energy of the pure [PVA:PEO] blend film is 0.2646 kg.m²/sec, and impact strength is 0.09155 kg/m². With the reinforcement by $CuCl_2.2H_2O$ at different weight ratios, a continuous linear decrease in both fracture energy and impact strength was seen, reaching it is minimum at 40wt% of $CuCl_2.2H_2O$. Then the fracture energy and impact strength were increased at 50wt% of added $CuCl_2.2H_2O$, as shown in Table 3. This decrease is due to the dependence of fracture energy on the weight ratios of the polymeric blend, the degree of interlinking between the polymers, and the nature and size of the polymer particles. Fracture energy

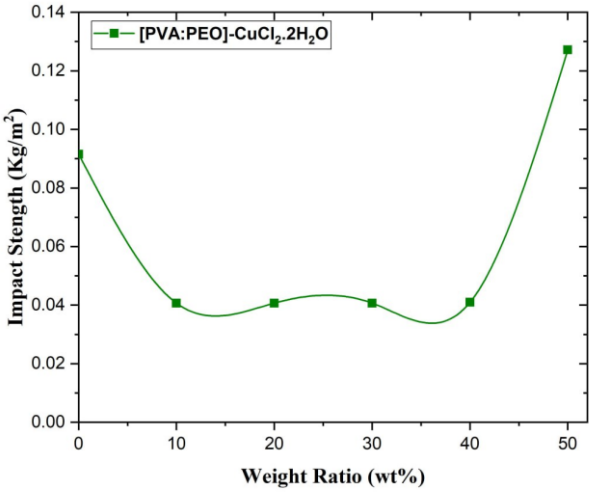

Fig. 6. Impact strength of pure [PVA:PEO] blend film and the films reinforced with $CuCl_2.2H_2O$ salt at different weight ratios.

Table 3. The value of the fracture energy and impact strength of pure [PVA:PEO] blend film and the film reinforced with $CuCl_2.H_2O$ at different weight ratios.

$CuCl_2.H_2O$ (wt%)	Distance (cm)	mass additive (g)	[PVA:PEO]-$CuCl_2.2H_2O$ Fracture energy (kg.m²/sec)	[PVA:PEO]- $CuCl_2.2H_2O$ Impact strength (kg/m²)
Pure [PVA:PEO]	30	90	0.2646	0.09155
10	30	40	0.1176	0.04069
20	30	40	0.1176	0.04069
30	30	40	0.1176	0.04069
40	30	40	0.1176	0.04069
50	30	12.5	0.3675	0.12716

decreases as the size of the particles becomes very small, this is attributed to the spread of small particles in the reinforced polymeric blend, which can act as sites for fine cracks and propagate fractures within the reinforced polymeric blend, the cause is the concentration of stresses. Additionally, fracture energy depends on the type of stress applied to the samples, manufacturing conditions, geometric shape, dimensions, and environmental conditions. Factors such as density, average molecular weight, and molecular weight distribution of the polymeric blend reinforced with $CuCl_2.2H_2O$ also affects mechanical properties. Density is positively correlated with material crystallinity; higher density generally indicates higher crystallinity due to the close packing and alignment of polymer chains. Consequently, the final product's properties, like elastic modulus increase with higher density, while fracture energy decreases with higher density [22, 24], which is in good agreement with previous research [25]. The increase in fracture energy and impact strength at 50 wt% of added $CuCl_2.2H_2O$, where the fracture energy is 0.3675 kg.m²/sec and the

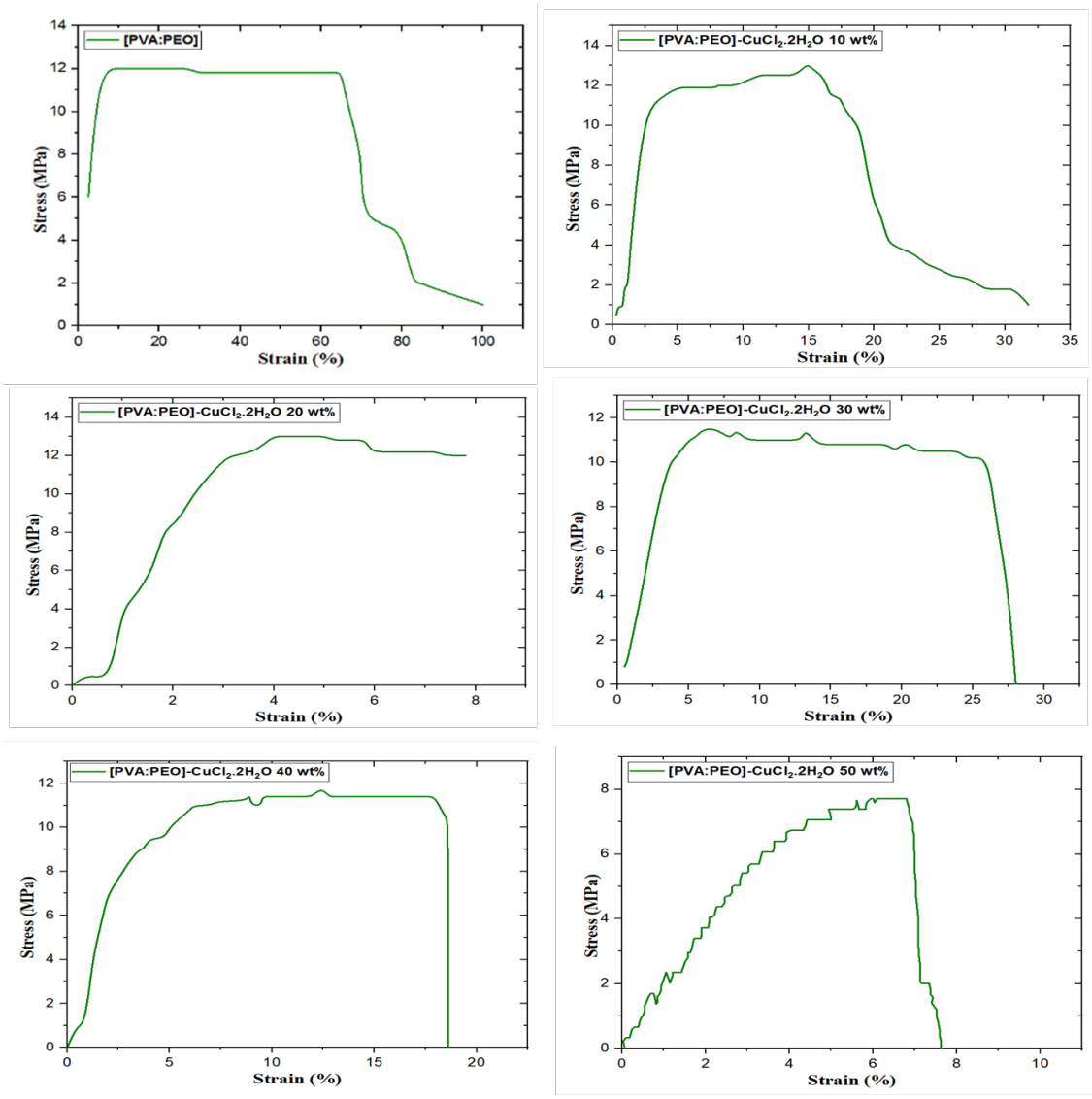

Fig. 7. Stress-strain curves of the pure [PEO:PVA] blend film and the films reinforced with $CuCl_2.2H_2O$ at different weight ratio.

impact strength is 0.12716 kg/m², is attributed to salt ratio that hinders cracks propagation and changes the direction and formation of cracks. These factors lead to improved resistance when $CuCl_2.2H_2O$ added at this ratio [26, 27]. The addition of $CuCl_2.2H_2O$ at 50 wt% in the [PVA:PEO] blend improved the mechanical properties of these films. Another reason for the increased fracture energy and impact strength at this ratio is that a significant portion of the energy applied to the sample is absorbed by the $CuCl_2.2H_2O$, thereby enhancing the material's resistance [28-30].

Tensile test were performed on polymeric blend films reinforced with $CuCl_2.2H_2O$ at different weight

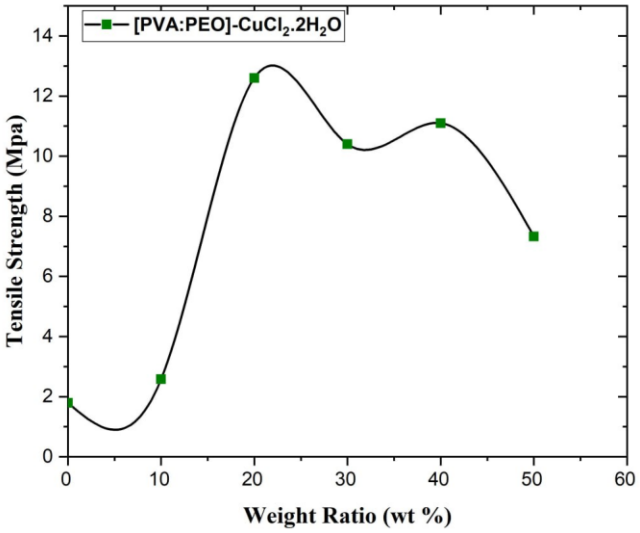

Fig. 8. Tensile strength of pure [PVA:PEO] blend films and the films reinforced with $CuCl_2.2H_2O$ at different weight ratios.

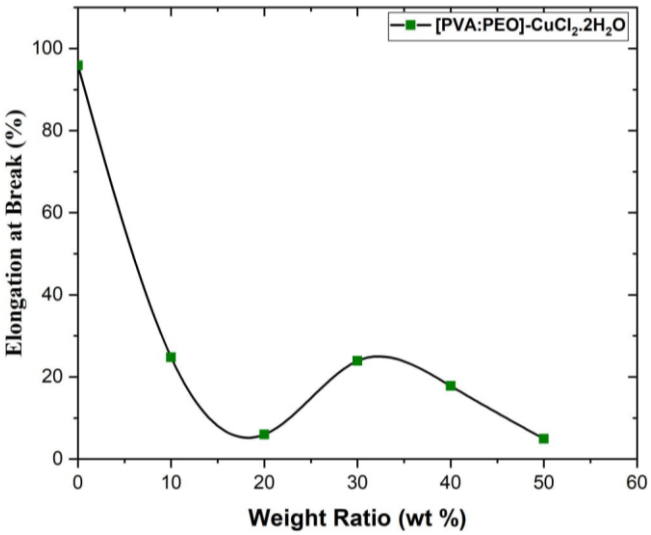

Fig. 9. Elongation at break for the pure [PVA:PEO] blend film and the films reinforced with $CuCl_2.2H_2O$ at different weight ratios.

ratios, as well as pure [PVA:PEO] blend film. Stress-strain curves were shown in Fig. 7. It is observed that the pure [PVA:PEO] blend film exhibits a region of elastic deformation characterized by a linear relationship between stress and strain. The Young's modulus can be represented by the slope of the linear region of the stress-strain curve. In this region, the polymeric material undergoes elastic deformation due to the stretching and elongation of the polymer chains without breaking their bonds. However, as the stress increases, the curve deviates from linear behavior due to the formation of cracks within the polymeric material. These cracks begin to grow and coalesce,

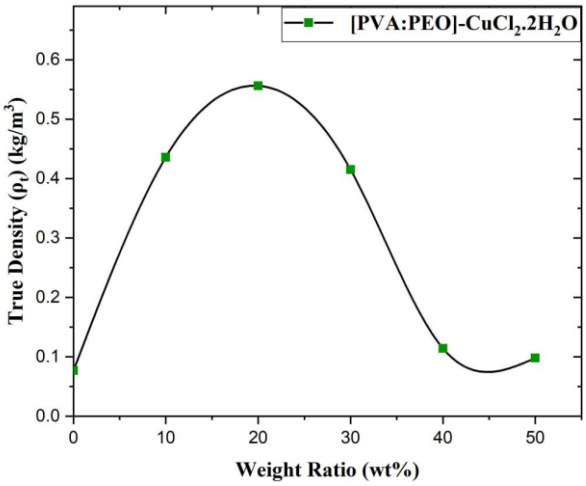

Fig. 10. True density of pure [PVA:PEO] blend film and film reinforced with $CuCl_2.2H_2O$ at different weight ratios.

Table 4. The values of the tensile strength and elongation at break of the pure [PVA:PEO] blend film and films reinforced with $CuCl_2.2H_2O$ at different weight ratios.

Weight ratio of additive $CuCl_2.2H_2O$ (wt%)	[PVA:PEO]-$CuCl_2.2H_2O$ Ultimate tensile strength (Mpa)	[PVA:PEO]-$CuCl_2.2H_2O$ Ultimate elongation at break (%)
Pure [PVA:PEO]	1.79	95.9
10	2.58	24.8
20	12.6	5.96
30	10.4	23.9
40	11.1	17.8
50	7.33	4.91

leading to larger and more pronounced fractures and ultimately resulting in sample failure [31]. In some cases, failure begins at external surfaces or at defects such as internal cracks, scratches, or indentations,which act as stres concentrators. These defects increases localized stress, leading to elevated internal cohesion strength of material. Consequently, the stress-strain curve will exhibit changes reflecting the onset of failure and the material's response to concentrated stresses. When the [PVA:PEO] blend film is reinforced with $CuCl_2.2H_2O$ at different weight ratios, different characteristics are observed in the resulting stress-strain curves, depending on the type of reinforcement material and its concentration [25, 32, 33]. Table 4 presents the tensile strength and elongation at break values determined from the stress-strain curves for all the blend films. It shoud be noted that the tensile strength value of the pure [PVA:PEO] blend film is 1.79 MPa, and the elongation at break value is 59,9%. However, after reinforcing the blend films with $CuCl_2.2H_2O$ at different weight ratios, it was observed that the tensile strength value increased irregularly

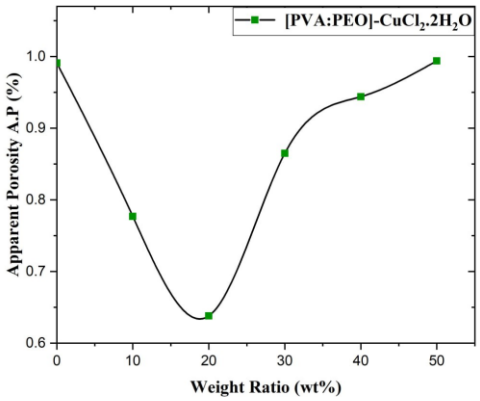

Fig. 11. Apparent porosity of the pure [PVA:PEO] blend film and the films reinforced with $CuCl_2.2H_2O$ at different weight ratio.

Table 5. The true density values for the pure polymeric [PVA:PEO] blend film and film reinforced $CuCl_2.2H_2O$ salt at different weight ratios.

Weight ratio of additive salt $CuCl_2.2H_2O$ (wt%)	[PVA:PEO]-$CuCl_2.2H_2O$ ture density ρ_t (g/cm^3)
Pure [PVA:PEO]	0.077
10	0.436
20	0.556
30	0.415
40	0.114
50	0.098

with an increase in the weight ratio of added $CuCl_2.2H_2O$. Conversely, the elongation at break value decreased irregularly with an increase in the weight ratios of added $CuCl_2.2H_2O$. The increase in the tensile properties value indicates that the added reinforced material interacts physically with the [PVA:PEO] blend [33, 34]. It also suggests that the added reinforced material is compaatible with the common added polymerization [22, 33], affecting the mechanical properties [35, 36]. The decrease in the tensile properties value, represented by the elongation at break for all the polymeric blend films, is due to weak interaction between the molecules as well as the lack of the interfacial adhesion in the tensile properties and the fragility of the composite [34, 36-38]. Figs. 8 and 9 show the tensile strength and elongation at break of all blend films.

True density results

The true density is calculated based on below equation [39]:

$$\rho_t = w_1 / (w_3 - w_2) \times D \quad (5)$$

where, ρ_t is true density (g/cm³). D show density of distilled water (g/cm³). w_1 displays weight of the dry sample (g). w_2 is weight of the sample when submerged in water (g). w_3 denotes weight of the sample after saturation with water (g).

As shown in Fig. 10, the true density of the pure [PVA:PEO] film is 0.077 g/cm³. After reinforcement by $CuCl_2.2H_2O$ at different weight ratios, an irregularly increase in true density was noted with an increase in the weight ratio of added salt. This increase is attributed to the chemical composition of the salt, which affects density at a given temperature [40]. Additionally, immersing the sample in water helps compact the granular components, leading to an increased packing density. However, an increase in density does not indicate full density of material, as increased density may result from reduced porosity [41, 42]. Table 5 shows the true density values for all the pure blend films.

Apparent porosity test results

The apparent porosity is calculated as follow [43]:

$$(A.P)\ \% = \frac{W_3 - W_1}{W_3 - W_2} \times 100\% \quad (6)$$

where, A.P is apparent porosity. w_1 shows weight of the dry sample (g). w_2 denotes weight of the sample when submerged in water (g). w_3 illustrates weight of the sample after saturation

Table 6. The apparent porosity values of the pure [PVA:PEO] blend film and films reinforced $CuCl_2.2H_2O$ at different weight ratios.

Weight ratio of additive salt $CuCl_2.2H_2O$ (wt%)	[PVA:PEO]- $CuCl_2.2H_2O$ apparent porosity (A.P) (%)
Pure [PVA:PEO]	0.991
10	0.777
20	0.638
30	0.865
40	0.944
50	0.994

with water (g).

As shown in Fig. 11, the apparent porosity of the pure [PEO:PVA] blend film is 0.991%. Upon reinforcement by $CuCl_2.2H_2O$ at different weight ratios, the apparent porosity decreased irregularly with an increase in the weight ratio of added salt. This decrease in apparent porosity is attributed to the blockage and packing of particles within the sample. Apparent porosity depends on three crucial factors: temperature, voids within the film, and pore formation. Open pores can release gases that affect these factors, thus offering an inverse effect [44, 45]. Additionally, the raw materials used in sample preparation significantly affect porosity by pressure during the process of water immersion of sample and the size and distribution

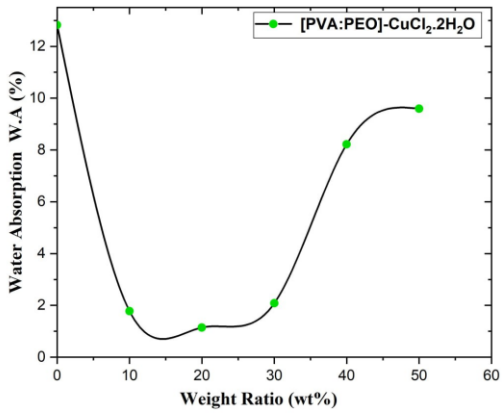

Fig. 12. Water absorbance of pure [PVA:PEO] blend film and the films reinforced with $CuCl_2.2H_2O$ at different weight ratios.

Table 7. The values of the water absorbance of the pure [PVA:PEO] blend film and films reinforced with $CuCl_2.2H_2O$ at different weight ratios.

Weight ratio of additive salt $CuCl_2.2H_2O$ (wt%)	[PVA:PEO]- $CuCl_2.2H_2O$ water absorbance W.A (%)
Pure [PVA:PEO]	12.823
10	1.781
20	1.146
30	2.082
40	8.222
50	9.590

of particles [46, 47]. Table 6 shows the apparent porosity values for all the blend films.

Water absorbance test result

The water absorbance calculated using the equation [48]:

$$(W.A)\ \% = \frac{W_3 - W_1}{W_1} \times 100\% \quad (7)$$

where, W.A is water absorbance. w_1 shows weight of the dry sample (g). w_3 denotes weight of the sample after saturation with water (g).

As shown in Fig. 12, the water absorbance of the pure [PVA:PEO] blend film is 12.823%. However, after reinforcement by $CuCl_2.2H_2O$ at different weight ratios, an irregularly decrease in water absorbance was observed with an increase in the weight ratio of added salt. This decrease in water absorbance is attributed to the enhancement in the liquid phase, resulting from the interaction of the film components with the solid phase. There is a phase relationship between water absorbance and porosity apparent [49-52]. Table 7 shows the water absorbance values for all blend films.

CONCLUSION

The thermal conductivity of pure [PVA:PEO] blend films, measured *via* the Lees disk method, decreased irregularly with increasing $CuCl_2.2H_2O$ content. However, values remained consistently low (0.12–0.25 W/m·K across all ratios), indicating intrinsic thermal insulation behavior. Pure blend (0 wt% salt) showed thermal conductivity of ≈ 0.25 W/m·K., which is suitable for low-cost thermal insulation panels in building materials. Compounds based on 10–20 wt% salt offered conductivity of ≈ 0.18 W/m.K, which is ideal for protective packaging for heat sensitive electronics (ASTM D5334). Compounds based on 30–50 wt% salt demonstrated a conductivity of ≈ 0.12 W/m.K. with potential for aerospace-grade lightweight insulation. The hardness factor increase from 0.3 GPa to 0.45 GPa at 10 wt% of salt, followed by irregular decline (0.35 GPa at 50 wt%). Fracture energy decreased at low salt ratios (0–20 wt%) but rebounded at 30–50 wt%, exceeding pure blends by 15%. Tensile strength fluctuated between 12–18 MPa, with no clear concentration dependency. Elongation at break declined inconsistently from 250% to 120%. Compounds based on 10–20 wt% salt (High Hardness) are suitable for high-durability adhesives in automotive assembly. Compounds based on 30–50 wt% salt (Improved Impact Resistance) are ideal for protective coatings in construction. Pure blend (High Elongation) has biomedical applications requiring flexibility, e.g., wearable sensors. Non-linear tensile behavior caused by phase separation and solution incorporate PEO-grafted nanoparticles to enhance interfacial bonding. Low salt content (0–20 wt%) and high porosity (10–15%) supports moisture-wicking textiles. High salt content (30–50 wt%) and low water absorption (<10%) is ideal for water-resistant coatings in marine environments.

CONFLICT OF INTEREST

The authors declare that there is no conflict of interests regarding the publication of this manuscript.

REFERENCES

1. Gao C, Wang F, Hu X, Zhang M. Research on the Analysis and Application of Polymer Materials in Contemporary Sculpture Art Creation. Polymers. 2023;15(12):2727.
2. Dwyer FP, Gyarfas EC, Rogers WP, Koch JH. Biological Activity of Complex Ions. Nature. 1952;170(4318):190-191.
3. Doettinger F, Yang Y, Karnahl M, Tschierlei S. Bichromophoric Photosensitizers: How and Where to Attach Pyrene Moieties to Phenanthroline to Generate Copper(I) Complexes. Inorganic chemistry. 2023;62(21):8166-8178.
4. Pallenberg AJ, Koenig KS, Barnhart DM. Synthesis and Characterization of Some Copper(I) Phenanthroline Complexes. Inorganic Chemistry. 1995;34(11):2833-2840.
5. Chen L, Lin Z. Polyethylene: Properties, Production and Applications. 2021 3rd International Academic Exchange Conference on Science and Technology Innovation (IAECST); 2021/12/10: IEEE; 2021. p. 1191-1196.
6. Yu Y, Huang Q, Zhou J, Wu Z, Deng H, Liu X, et al. One-step extraction of high-purity CuCl2·2H2O from copper-containing electroplating sludge based on the directional phase conversion. J Hazard Mater. 2021;413:125469.
7. Kock WE. A hologram form of bistatic radar or sonar. Proc IEEE. 1969;57(1):100-100.
8. Almashhadani NJH. Weathering effect Weathering effect on the mechanical properties of PEO/PVA blends. Iraqi Journal of Science. 2021:1879-1892.
9. Bama GK, Devi PI, Ramachandran K, Garg AB, Mittal R, Mukhopadhyay R. Structural and Thermal Properties of PVA and Its Composite with CuCl[sub 2]. AIP Conference Proceedings: AIP; 2011.
10. Tweissi M, Khoshman JM, Miqdad H, Adaileh A. Determination of Lorenz number of composite films based on copper chloride(II) in polyvinyl alcohol matrix. Plastics, Rubber and Composites: Macromolecular Engineering. 2024;53(1):36-42.
11. Xiao Y, Liu S, Zhou J, Zhang S, Li Z, Xiong S, et al. Lightweight, strong, and thermally insulating polybenzoxazine aerogel thermal protection composites for antioxidant ablation long to 1800 s. Composites Part B: Engineering. 2023;266:111045.

12. Nasar G, Khan MS, Khalil U. A Study on Structural, Mechanical and Thermal Properties of Polymer Composites of Poly(vinyl alcohol) with Inorganic Material. Macromolecular Symposia. 2010;298(1):124-129.
13. Salman SA, Bakr NA, Jwameer MR. Effect of Annealing on the Optical Properties of (PVA-CuCl) Composites. International Letters of Chemistry, Physics and Astronomy. 2016;63:98-105.
14. Kalfoglou NK. Compatibility of poly(ethylene oxide)–poly(vinyl acetate) blends. Journal of Polymer Science: Polymer Physics Edition. 1982;20(7):1259-1267.
15. Sun Z, Yu H, Feng Y, Feng W. Application and Development of Smart Thermally Conductive Fiber Materials. Nanomaterials (Basel, Switzerland). 2024;14(2):154.
16. Kuekha M R, Salman S, Mhammed Ahmed D. Study of Some physical properties of (PVA-CuCl) composite films. Journal of Garmian University. 2019;6(SCAPAS Conferance):38-45.
17. Arkis E, Cetinkaya H, Kurtulus I, Ulucan U, Aytac A, Balci B, et al. Characterization of a Pearlescent Biaxially Oriented Multilayer Polypropylene Film. Chemistry & Chemical Technology. 2015;9(1):77-84.
18. Hussein BH, Hassun HK, Maiyaly BKH, Aleabi SH. Effect of copper on physical properties of CdO thin films and n-CdO: Cu / p-Si heterojunction. Journal of Ovonic Research. 2022;18(1):37-34.
19. Abdel-Kader MH, Alharby TS, Alamri SN. Enhancement of structural, morphological, thermal, optical and mechanical characteristics of PVA/PEO blends based on acetate fillers and infrared laser irradiation. Radiat Phys Chem. 2025;229:112488.
20. Eslami B, Ghasemi I, Esfandeh M. Using Pegylated Graphene Oxide to Achieve High Performance Solid Polymer Electrolyte Based on Poly(ethylene oxide)/Polyvinyl Alcohol Blend (PEO/PVA). Polymers. 2023;15(14):3063.
21. Abed AH, Ma'atook EN, Aziz KK, Al-zahra MJA. Antibiotic Susceptibility of Bacterial Wound Infection: A Cross Sectional Study. International Journal of Medical Science and Clinical Research Studies. 2023;03(07).
22. Meyers MA, Chawla KK. Mechanical Behavior of Materials: Cambridge University Press; 2008 2008/11/06.
23. Nur Farahana R, Supri Abdul G, Teh Pei L, Yeoh Cheow K. Effects of Poly(vinylchloride)-Maleic Anhydride as Coupling Agent on Mechanical, Water Absorption, and Morphological Properties of Eggshell Powder Filled Recycled High Density Polyethylene/Ethylene Vinyl Acetate Composites. Journal of Advanced Research in Applied Sciences and Engineering Technology. 2022;28(1):33-43.
24. Alghamdi HM, Abutalib MM, Mannaa MA, Nur O, Abdelrazek EM, Rajeh A. Modification and development of high bioactivities and environmentally safe polymer nanocomposites doped by Ni/ZnO nanohybrid for food packaging applications. Journal of Materials Research and Technology. 2022;19:3421-3432.
25. Ragab HM. The influence of graphene oxide on the optical, thermal, electrical, and dielectric properties of PVA/PEO composite. Journal of Materials Science: Materials in Electronics. 2022;33(25):19793-19804.
26. Yildirim Y, Saltan F, Şirin K, Küçük VA. Thermal decomposition kinetics and mechanical analysis of boron carbide-reinforced polymer nanocomposites. Polymer Engineering and Science. 2025;65(5):2308-2322.
27. Silva ELd, Reis CA, Vieira HC, Santos JXd, Nisgoski S, Saul CK, et al. Evaluation of Poly(Vinyl Alcohol) Addition Effect on Nanofibrillated Cellulose Films Characteristics. Cerne. 2020;26(1):1-8.
28. Pedroni LG, Soto-Oviedo MA, Rosolen JM, Felisberti MI, Nogueira AF. Conductivity and mechanical properties of composites based on MWCNTs and styrene-butadiene-styrene block™ copolymers. J Appl Polym Sci. 2009;112(6):3241-3248.
29. Yan S, Zhang F, Luo L, Wang L, Liu Y, Leng J. Shape Memory Polymer Composites: 4D Printing, Smart Structures, and Applications. Research (Washington, DC). 2023;6:0234-0234.
30. Dasari A, Yu Z-Z, Mai Y-W. Introduction: Toward Multi-functionality. Engineering Materials and Processes: Springer London; 2016. p. 1-4. http://dx.doi.org/10.1007/978-1-4471-6809-6_1
31. Yu XD, Malinconico M, Martuscelli E. Highly filled particulate composites enhancement of performances by using compound coupling agents. Journal of Materials Science. 1990;25(7):3255-3261.
32. Jabur AR, Abdulmajeed MH, Abd SY. Effect of copper chloride salt($CuCl_2$) addition on DC,AC conductivity and tensile strength of PVA electrospun polymeric film. AIP Conference Proceedings: AIP Publishing; 2019. p. 020016.
33. Koduru HK, Bruno L, Marinov YG, Hadjichristov GB, Scaramuzza N. Mechanical and sodium ion conductivity properties of graphene oxide–incorporated nanocomposite polymer electrolyte membranes. J Solid State Electrochem. 2019;23(9):2707-2722.
34. Saleh NAM, A. Salman DS. Thermal Properties of Manganese Chloride Salt Reinforced [PVA: PVP] Blend Films. Neuroquantology. 2021;19(9):126-131.
35. Mahmood HS, Habubi NF. Structural, mechanical and magnetic properties of PVA-PVP: iron oxide nanocomposite. Appl Phys A. 2022;128(11).
36. Mahmood HS, Habubi NF. Physical Properties of PVA:PVP blend reinforced by MWCNT. Journal of Physics: Conference Series. 2022;2322(1):012068.
37. Al-Ramadhan Z, Algidsawi AJK, Hashim A, Aslan MH, Oral AY, Özer M, et al. The D.C Electrical Properties of (PVC-Al2O3) Composites. AIP Conference Proceedings: AIP; 2011.
38. Habubi N, Mahmood HS. Mechanical and Antibacterial Activity of Biodegradable Na-CMC: PVA Reinforced with Al_2O_3 Nanoparticles. International Journal of Nano and Biomaterials. 2024;1(1).
39. Jakić M, Santro A, Zečić E, Perinović Jozić S. Thermal Analysis of the Biodegradable Polymer PVA/PEO Blends. Tehnički glasnik. 2024;18(2):224-228.
40. Guirguis OW, Moselhey MTH. Thermal and structural studies of poly (vinyl alcohol) and hydroxypropyl cellulose blends. Natural Science. 2012;04(01):57-67.
41. Dzhardimalieva GI, E. Uflyand I. Supramolecular Chemistry of Polymer Metal Chelates. Springer Series in Materials Science: Springer International Publishing; 2018. p. 761-897.
42. Gupta B, Agarwal R, Sarwar Alam M. Preparation and characterization of polyvinyl alcohol-polyethylene oxide-carboxymethyl cellulose blend membranes. J Appl Polym Sci. 2012;127(2):1301-1308.
43. Lv K, Wan H, Qi C, Wang W, Liu X, Zhang L, et al. Integrating AI and material science: MXene synthesis, preparation, and applications. AI & Materials. 2025.
44. Hosseini Akbarnejad R, Daadmehr V, Rezakhani AT, Shahbaz Tehrani F, Aghakhani F, Gholipour S. Catalytic Activity of

the Spinel Ferrite Nanocrystals on the Growth of Carbon Nanotubes. Journal of Superconductivity and Novel Magnetism. 2012;26(2):429-435.
45. Liu Z-X, Liu D-Z, Zhang C-H, Wang W-J, Huang H, Yang S-G. Stabilize and Reinforce Hydrogen-Bonded Polymer Complex Elastic Fiber by Catechol Chemistry and Coordination. Chin J Polym Sci. 2023;41(12):1846-1855.
46. Samad A. Manufacture of Refractory Brick from Locally Available Red Clay Blended with White Portland Cement and Its Performance Evaluation. International Journal of GEOMATE. 2021;20(80).
47. Behera SK, Barpanda P, Pratihar SK, Bhattacharyya S. Synthesis of magnesium–aluminium spinel from autoignition of citrate–nitrate gel. Mater Lett. 2004;58(9):1451-1455.
48. Agarwal R, Alam MS, Gupta B. Polyvinyl alcohol-polyethylene oxide-carboxymethyl cellulose membranes for drug delivery. J Appl Polym Sci. 2013;129(6):3728-3736.
49. Bhavikatti AM, Kulkarni S, Lagashetty AK. Microwave Synthesis of Nickel Ferrite: Structure, Morphology and Bonding. Material Science Research India. 2007;4(2):459-463.
50. Alotaibi BM, Atta A, Atta MR, Abdeltwab E, Abdel-Hamid MM. Modifying the optical properties of hydrogen-beam-irradiated flexible PVA polymeric films. Surface Innovations. 2024;12(1-2):84-95.
51. Weng C-H, Tsai C-Z, Chu S-H, Sharma YC. Adsorption characteristics of copper(II) onto spent activated clay. Sep Purif Technol. 2007;54(2):187-197.
52. Qin F, Shi Q, Zhou G, Liu X, Chen L, Du W, et al. Influence of powder particle size distribution on microstructure and mechanical properties of 17-4 PH stainless steel fabricated by selective laser melting. Journal of Materials Research and Technology. 2023;25:231-240.